2013 IEEE/RSJ International Conference on
Intelligent Robots and Systems (IROS)
November 3-7, 2013. Tokyo, Japan

Discrete-Time Series Identification of Sliding Dynamic Friction in Industrial Robotic Joints

Michael Ruderman

Abstract— **In this paper, the discrete-time series identification of dynamic friction in actuated robotic joints during the sliding regime is proposed. Considering the friction lag as a first-order time delay element behind the static friction nonlinearity a reasonable approximation of friction dynamics in sliding is proposed. The regression signal model is derived based on a discrete-time transformation of motion dynamics with nonlinear friction. A robust identification scheme is formulated in the Least-Squares (LS) sense by using an appropriate set of model-related regressors. Further, the related Recursive-Least-Squares (RLS) formulation is provided. The proposed modeling and identification are evaluated experimentally by the offline and online parameter estimation. For these purposes the first vertical rotary joint of the base of a standard industrial robotic manipulator has been used in laboratory environment.**

Index Terms— **Dynamic friction, time-series modeling, sliding dynamics, robotic joint, recursive identification, parameter estimation, industrial robotics, friction lag, nonlinearities**

I. INTRODUCTION

High-performance control of robotic joints requires an appropriate modeling and identification of dynamic behavior. Here the nonlinear effects of dynamic friction play one of the key roles when describing the actuated joint motion. Due to time- and load-variant effects, the online identification and adaptive methods to overcome friction are desirable in applications. However, these can be cumbersome due to non-trivial friction phenomena which are not directly detectable.

Several works have investigated adapting the modeled friction for control. A recursive least-squares algorithm has been applied to a simplified static friction model with individual Coulomb and viscous friction coefficients for opposite motion directions in [1]. This approach allowed to design an adaptive friction compensator for DC-motor drives. Later, an auto-tuning of feedforward friction compensator has been proposed in [2] where, more advanced, the dynamic LuGre friction model has been involved in the adaptation scheme.

Generally, all types of high-accuracy positioning systems, including robotics, require an explicit consideration of friction effects. Various modeling and compensation techniques have been proposed to this matter in the last two decades. In [3], the friction compensator is based on the experimental friction model and allows to compensate for non-modeled nonlinear friction. Friction identification and compensation in robotic manipulators have been addressed in [4] using a single-state dynamic friction model and evaluating the same method on two different type (micro- and macro-scale) manipulators. The experimental robot identification and optimal excitation required therefor have been addressed in [5]. In [6], a high precision position control using an adaptive friction compensation has been presented which is based on the regression friction modeling proposed former in [7]. The modeling and identification of nonlinear friction in a serial manipulator have been addressed in [8] in frame of an industrial robot control. In [9], a simple technique to identify the dynamic friction using the frequency response functions obtained from the measurements and numerical simulations has been proposed. The method has been applied later in [10] for an observer-based friction control design. A simultaneous identification of linear parameters of the drive system and nonlinear rolling friction has been addressed in [11]. Further, a detailed model-based analysis of rolling friction has been provided in [12]. The above mentioned works establish the importance of treating friction effects in the controlled machines and mechanisms and diversity of methods developed therefor.

Often, the challenge of dynamic friction modeling relates to a straightforward identification during the operation, that is crucial for multiple applications. Often it is worthwhile to apply a simplified friction model, without losing the faithfulness and generality, which could provide a simple way to determine a possibly small set of free parameters. The objective of this paper is to demonstrate one practical solution of describing and identifying the sliding dynamic friction in industrial robotic joints. The proposed method bases on the discrete-time series modeling and the fact that the sliding friction dynamics exhibits a characteristic lag between the relative velocity and friction response. Further, it should be noted that the considered friction dynamics restricts oneself to the sliding regime [13] only. That is the pre-sliding nonlinear (hysteresis) friction behavior, which can be crucial in micro-displacement ranges, is out of scope of this work. However, the proposed idea of discrete-time series representation of dynamic friction, similar like another approach elaborated in [7], can be motivating for further efforts towards more general and easy-identifiable friction models reliable for applied control in robotics and mechatronics.

II. MODELING OF DYNAMIC FRICTION IN ROBOTIC JOINTS

A. Single-mass joint dynamics with nonlinear friction

In order to analyze the dynamic friction in robotic joints a simplified single (lumped) mass approach can be considered as schematically shown in Fig. 1. This case, a concentrated

M. Ruderman is with Department of Computer Science and Engineering, Nagoya Institute of Technology, Gokiso, Showa, Nagoya, 466-8555 Japan ruderman.michael@nitech.ac.jp

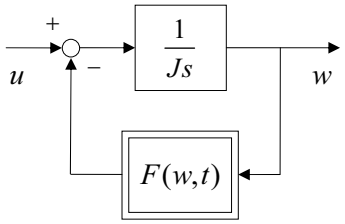

Fig. 1. Single lumped-mass joint dynamics with nonlinear friction

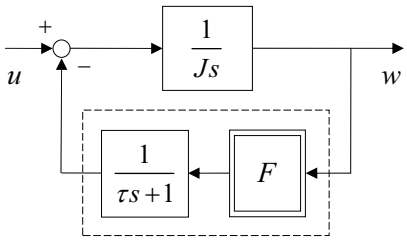

friction with lag

Fig. 2. Approximation of sliding dynamics with friction lag

moving mass (inertia) J is accelerated by a general joint input force (torque) u. Mostly, the latter can be assumed as an available control quantity which is proportional to the active motor current of the joint actuator. The induced relative velocity w is considered to be mainly damped by the feedback friction $f(\cdot)$. The latter can be assumed as a dynamic nonlinear map of relative velocity onto the dissipative force (torque) which is acting tangentially and in opposite direction to the induced relative motion. In general case, the dynamic friction map has to be considered as time-variant due to non-constant properties of frictional interfaces, these depending on the environmental and operation conditions. The latter include, among others, the thermal effects, normal mechanical loads, dwell times, and wearing of contacting mechanisms. All these effects are mostly of non-deterministic nature and are extremely difficult, if at all possible, to be included into a manageable friction model suitable for control.

Note that the simplified single lumped-mass modeling does not consider the robot joint elasticities and residual feedback manipulator dynamics (see e.g. [14] for details). Recall that the impact of nonlinear elasticities and residual (dynamic) joint loads can be also regarded as a coactive input disturbance as shown e.g. in [15]. However, this type of joint forces is out of scope of the recent work. Further, it is worth noting that various modeling approaches available from the literature, e.g. [7], [16], [12], can be used for describing the dynamic friction as well.

B. Sliding dynamics with frictional lag

Since the sliding dynamics is characterized by a lag in friction force relative to sliding velocity (see [13] for details) an approximation of sliding dynamics can be achieved by introducing a time lag transfer element behind the friction nonlinearity. In other words, the output of static friction nonlinearity F will undergo the first-order time delay transition. Simple case, the corresponding time constant τ determines the impact of friction lag so that the latter is captured by

$$\tau \dot{f}(t) + f(t) = F(w). \tag{1}$$

The resulted approximation of dynamic friction f with lag is illustrated by the block diagram in Fig. 2.

It can be shown that using the block transformations one obtains the equivalent system structure described by the following differential equation

$$J\tau \ddot{w}(t) + J\dot{w}(t) + F\big(w(t)\big) = u(t) + \tau \dot{u}(t). \tag{2}$$

Important to note is that the resulted second-order velocity dynamics, on the left-hand side of (2), is always positively damped due to non-zero inertial term. Furthermore, it can be seen that the second-order velocity dynamics does not tend to an oscillating behavior since the restoring term $F(\cdot)$ implies a discontinuity at zero crossing.

Recall that $F(\cdot)$ constitutes a velocity-dependent static friction map which, simple case, can be represented by combining the constant Coulomb and linear viscous friction denoted by F_c and σ correspondingly. More advanced, the static nonlinear friction is captured by the well-known Stribeck characteristic curve

$$F(w) = \operatorname{sgn}(w)\Big(F_c + (F_s - F_c)\exp\Big(-\Big|\frac{w}{V_s}\Big|^{\delta}\Big)\Big) + \sigma w. \tag{3}$$

The static Stribeck curve is upper bounded by the adhesion (also denoted as stiction) friction force F_s and low bounded by the Coulomb friction force. The exponential factors V_s and δ, which determine the nonlinear curvature of Stribeck function, are denoted as Stribeck velocity and Stribeck shape factor correspondingly. Further it is worth noting that depending on the case-specific friction characteristics the shape factor can be positive or negative as well.

III. DISCRETE-TIME SERIES MODEL

In order to identify the nonlinear joint dynamics with friction a discrete-time series model is derived in terms of a well-known regression signal representation. Using a discrete-time approximation of differential terms by means of the finite difference equations the parameters of system dynamics (2) are transformed into the corresponding regression parameters which should be identified. The transformation steps required for calculation are as following:

$$\begin{aligned}
\dot{x}(t) &\cong \big(x(k) - x(k-1)\big)/T_s, \\
\ddot{x}(t) &\cong \big(x(k) - 2x(k-1) + x(k-2)\big)/T_s^2, \\
a_1 &= \big(J\tau + JT_s\big)/\big(J\tau + JT_s + \sigma T_s^2\big), \\
a_2 &= J\tau/\big(J\tau + JT_s + \sigma T_s^2\big), \\
b_0 &= \big(T_s^2 + \tau T_s^2\big)/\big(J\tau + JT_s + \sigma T_s^2\big), \\
b_1 &= \tau T_s^2/\big(J\tau + JT_s + \sigma T_s^2\big), \\
c_1 &= F_c T_s^2/\big(J\tau + JT_s + \sigma T_s^2\big), \\
d_1 &= F_s T_s^2/\big(J\tau + JT_s + \sigma T_s^2\big).
\end{aligned}$$

Here the finite sampling time is denoted by T_s and the corresponding signal to be transformed is denoted by x.

Using the introduced regression parameters and solving the dynamic equation (2), which is first transformed into the discrete-time representation, results in

$$\begin{aligned} w(k) &= a_1\, w(k-1) - a_2\, w(k-2) + b_0\, u(k) - b_1\, u(k-1) \\ &\quad -c_1\, g\big(w(k-1)\big) - d_1\, h\big(w(k-1)\big)\,. \end{aligned} \tag{4}$$

Here the static nonlinear functions

$$g(w) = \operatorname{sgn}(w)\left(1-\exp\left(-\left|\frac{w}{V_s}\right|^{\delta}\right)\right), \tag{5}$$

$$h(w) = \operatorname{sgn}(w)\exp\left(-\left|\frac{w}{V_s}\right|^{\delta}\right) \tag{6}$$

of joint velocity constitute the regressors related to the Coulomb and adhesion friction forces.

Note that since the exponential Stribeck factors are nonlinear in (5) and (6) they should be excluded from the regression parameters and have to be assumed as constants determined beforehand[1]. By doing this, it can be assumed that the exponential shape factors V_s and δ characterize rather the structural friction properties which rely on the geometries and texture of contacting surfaces. Thus, they can be considered as less time-variant than the residual Stribeck parameters. This appears as a sufficiently reasonable relaxation since the spatial, thermal, and load-dependent conditions bear the main influence on the frictional coefficients F_s, F_c, and σ. Further, it should be noted that normal case the nonlinear regressors (5), (6) are the static functions of instantaneous velocity at k. However, since $w(k)$ constitutes the unknown variable of regression model its previous discrete-time value at $k-1$ is assumed as argument in equation (4).

Now let us analyze the impact of the above assumption on the model accuracy of predicting the joint dynamics with nonlinear friction. The impact of previous discrete-time velocity value on computing the nonlinear friction can be demonstrated by means of a schematic representation given in Fig. 3. Assume that the input quantity u changes continuously its sign and the induced relative velocity w follows it subsequently, while being lagged behind due to inertial motion. The use of the previous velocity value is not critical when its sign at i-th and $(i-1)$-th instants remains the same. This is evident since the static nonlinear friction map given by (5) and (6) depends strictly on the motion direction, but at the same time has a quite smooth progression at unidirectional motion. However, once the velocity sign changes, e.g. see the instants $k-1$ and k in Fig. 3, the friction terms will transiently contribute to the overall motion dynamics with a spurious sign and that until the next sampling step $k+1$. Analyzing the dynamic equation (4) it can be recognized that both the propulsion input and inertial motion terms can mitigate this transient discrepancy in computed friction to a certain degree. However, if the motion reversal occurs at sufficiently slow (quasi-static) conditions, the use of a previous discrete-time velocity value can provoke certain distortions in properly determining the motion reversal state.

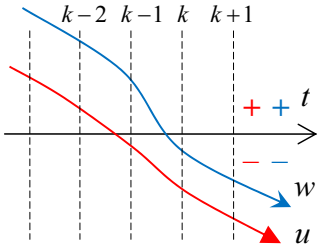

Fig. 3. Schematic representation of the sampled values at motion reversal

[1]This is valid since a linear regression model as in (4) is assumed. In case a nonlinear regression model is used also the exponential Stribeck factors can be explicitly considered for the online estimation. This is, however, out of scope of this work.

IV. OFFLINE AND ONLINE IDENTIFICATION

A. Least-squares formulation

Since the discrete-time series model (4) is linear in parameters its identification can be formulated in a 'classical' least-squares (LS) sense

$$W = XP + E. \tag{7}$$

Here the output and regressor values, W and X correspondingly, are assumed to be observable. Recall that the model regressors arise according to the discrete-time dynamics described before in Section III. The vector of model errors is denoted by E and P is the vector of linear model parameters to be determined. In order to find the least-squares best fit one should minimize the objective function

$$\min_P \frac{1}{2}\,||XP - W||. \tag{8}$$

The partial derivative of the objective function with respect to the parameters will be set to zero and yield the well-known equation of the LS estimate

$$\hat{P} = (X^T X)^{-1} X^T W\,. \tag{9}$$

For instance, the dynamic velocity response is obtained within numerical simulation by means of a persistent excitation through the low-pass filtered band-limited white noise. The performed LS parameter estimation yields the best fit of the discrete-time series model (4) whose response is shown in Fig. 4 together with the identification data. Here it is worth noting that the simulated identification data has been

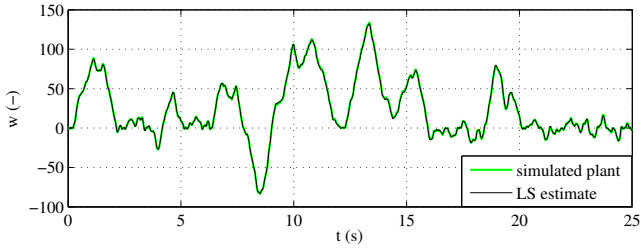

Fig. 4. Simulated and offline (LS) estimated output velocity

obtained by using the numerical model shown in Fig. 2 and not the regression model (4). The numerical model has been implemented using a fixed-step solver at 1 kHz rate. The identification data used for the LS fit has been collected equidistantly with the sampling time set to 10 ms.

B. Use of Recursive-Least-Squares (RLS) method

In terms of an online model identification a recursive algorithm [17] updates the estimate of parameter vector at each iteration step so that

$$\hat{P}(k) = \hat{P}(k-1) + \gamma\big(w(k) - \hat{w}(k)\big). \tag{10}$$

Here γ constitutes a correction vector at discrete time instant k and w is the measurable system output. Note that the model prediction is computed based on the parameter estimate at the previous time instant $k-1$ so that $u(k) \times \hat{P}(k-1) \rightarrow \hat{w}(k)$.

Using the well-known recursive least square (RLS) algorithm, first introduced in [18], one obtains the parameters update by evaluating the following equation

$$\hat{P}(k) = \hat{P}(k-1) + R(k)X(k)e(k)\,. \tag{11}$$

The prediction error is captured by $e = w - \hat{w}$ and X constitutes the vector of corresponding regressors. Note that the correction factor in (11) is determined by

$$\gamma(k) = R(k)X(k) = \frac{R(k-1)X(k)}{X^T(k)R(k-1)X(k) + \lambda}\,, \tag{12}$$

where R is a $n \times n$ covariance matrix, assuming n is the number of parameters to be identified. At each step of recursive algorithm the update of covariance matrix is computed by

$$R(k) = \frac{1}{\lambda}\left(I - \gamma(k)X^T(k)\right)R(k-1)\,, \tag{13}$$

where I is the identity matrix. Further it is worth noting that (12) and (13) imply the forgetting factor $0 < \lambda \leq 1$ which underweights the past measurements with respect to the current data. Note that $\lambda = 1$ corresponds to the original RLS in which all former observations contribute equally to the parameter estimate independently of the history.

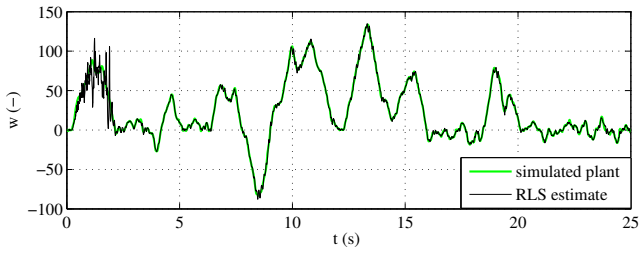

Fig. 5. Simulated and online (RLS) estimated output velocity

Using the same vector of regressors as mentioned in Section IV-A the RLS estimate starts by zero parameter initialization having R_0 at $k = 0$ set to a large-valued diagonal matrix. The simulated and RLS estimated output velocities are shown in Fig. 5. Here the same input-output data as used before for the LS fit are applied. It can be seen that the main transient oscillations vanish at time $t > 4$ s and the predicted output velocity converges towards the simulated value.

V. EXPERIMENTAL EVALUATION

A. Industrial robotic manipulator

The experimental evaluation of the proposed modeling and identification approach is performed on a standard industrial robotic manipulator with six rotary joints. The first vertical base-joint depicted in Fig. 6 is taken into consideration, since this moves the largest inertial mass of the overall robotic manipulator and is equipped by a large-scale gearing mechanism with considerable impact of friction. At the same

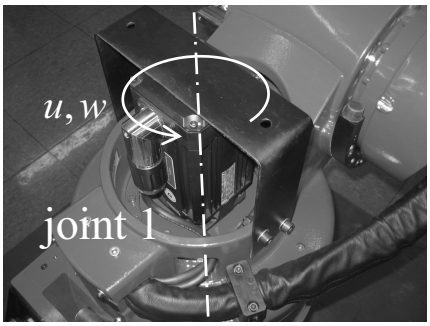

Fig. 6. First vertical base-joint of industrial robotic manipulator

time, the first vertical base-joint has no direct impact of gravity and can be actuated over the total operation range in a particular (vertical) arm configuration which is nearly free of coriolis and centrifugal terms. For more details about the employed experimental robotic system see [19], [20].

B. System excitation and data collection

The experimental data, used for the offline and online identification, have been collected during the closed loop control experiments, where a smooth multi-sinus (0.01–1 Hz) reference velocity is tracked by the industrial robot controller set to a single joint operation mode. The joint velocity varies between 1 deg/s and 20 deg/s and exhibits frequent motion reversals (see further in Section V-D) which are significant for dynamic friction behavior. The controlled motor current i and angular joint velocity w are readout from the industrial controller through an external TCP/IP-based interface. The corresponding input joint torque, depicted in Fig. 7, is computed from the measured motor current by $u = Ki$, where the linear factor K includes the nominal motor torque constant and inverse gear reduction ratio. Inspecting the close-up views on the top of Fig. 7 it can be seen that the available input signal is not smooth due to the time discretization and signal quantization effects. Further, it should be noted that the digital data processing, on the part of the robot controller, and the TCP/IP communication interface do not allow for a proper real-time data collection. These aspects of a non-deterministic sampling time will be further addressed in Section V-D, when evaluating the time-series model.

C. Pre-estimation of Stribeck curve

Before applying the discrete-time series identification of regression model the Stribeck function curvature has been

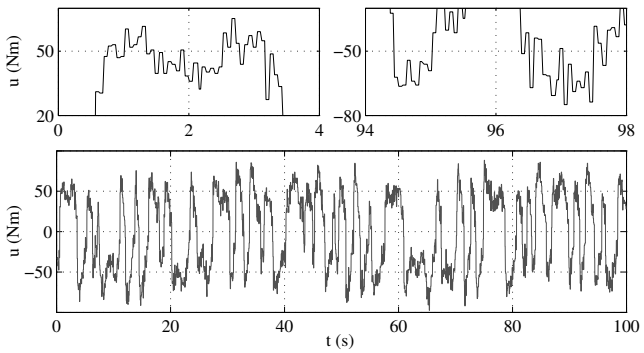

Fig. 7. Applied input joint torque signal with close-up views

pre-estimated from experiments. This is done in order to determine the exponential Stribeck factors excluded from the estimate as mentioned before in Section III. The Stribeck curve is fitted on the averaged support points of the joint velocity collected during the bidirectional quasi-static drive experiments. Due to the exponential parameter contribution the nonlinear curve fitting algorithm, the Levenberg-Marquardt, has been applied. These results have been former reported in [21]. Here the determined Stribeck curve is depicted in Fig. 8 over the measurements (mean values with corresponding spread) just for the sake of completeness.

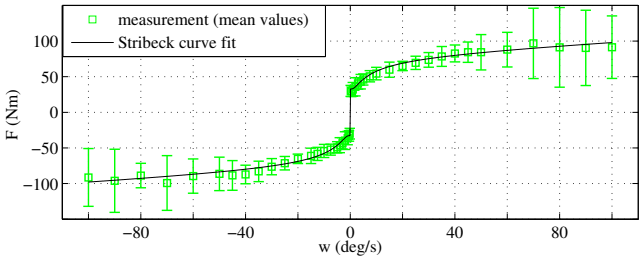

Fig. 8. Stribeck curve from bidirectional quasi-static drive experiments

D. Offline identification results

The controlled joint velocity response to the system excitation described before in Section V-B is shown in Fig. 9 together with the LS model fit obtained offline by use of the total identification data set. It can be seen that

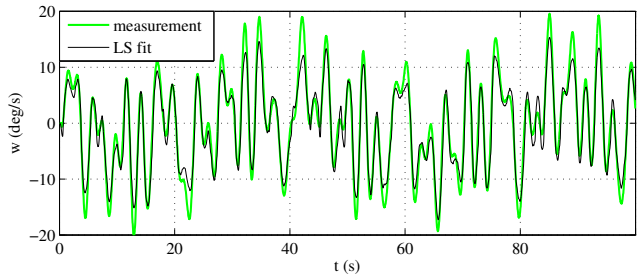

Fig. 9. Measured and offline identified robot joint velocity

despite the LS best fit the model prediction exposes several outliers, in particular at higher velocity peaks. On the one hand, it can be attributed to the simplification of sliding friction dynamics which is undertaken in Section II-B. On the other hand, a poor sampling quality of the data provides an additional source of estimate uncertainties. To expose this aspect consider the evaluated sample time during the identification experiments as depicted in Fig. 10. Note that the shown sample time of data collection is defined by $T_s = t(i) - t(i-1)$ and that for the overall set of readout data. From Fig. 10 one can recognize that despite an explicit

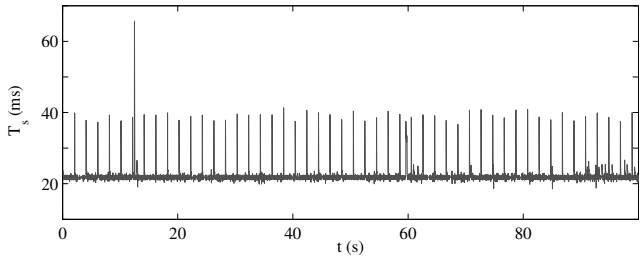

Fig. 10. Evaluated sample time during the identification experiments

average value (about 22 ms) the sample time is subject to a periodic pattern of different outliers. These indicate an apparent latency in the digital data processing and can amount almost up to twice of the average sample time. It is evident that due to nondeterministic corruption of the discrete-time signal series the identification data mismatches the modeled dynamics to a larger extend, even if the ratio between deterministic and corrupted data samplings remains still relative low.

E. Online identification results

The same identification data has been used to estimate the parameters of discrete-time series model online, i.e. by applying the RLS method as in Section IV-B. The input and output data are sequently proceeded to the identification algorithm without additional filtering or interpolation steps.

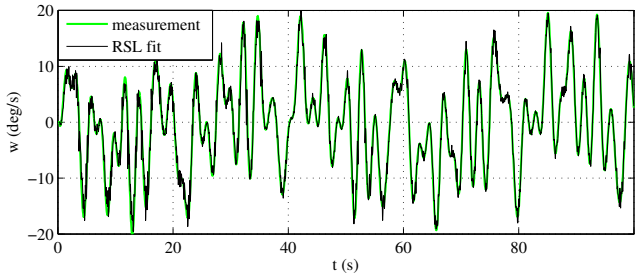

Fig. 11. Measured and online identified robot joint velocity

The measured and online-identified robot joint velocities are depicted about each other in Fig. 11. It can be seen that after the RLS estimate passes several transient oscillations, an apparent match between the model and measurement appears which is higher than this of the offline LS estimate. Here it is important to note that due to assumed high process and measurement noise the forgetting factor has been set to a low value $\lambda = 0.85$ which means a high forgetting

ratio. The corresponding convergence of model parameters is visualized in Fig. 12. It can be recognized that all six parameter trajectories proceed towards their stationary end-values after they have been initialized in zero. However, there are certain residual parameter fluctuations which are conditioned by the data quality and impact of forgetting factor. One can realize that, in particularly, the progress of b_0 and b_1 is subject to an oscillating pattern. This comes as not surprising in regard to non-smoothness of the associated input time series.

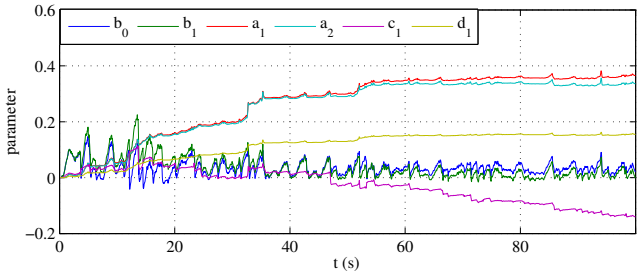

Fig. 12. Parameter convergence of RLS identification

VI. CONCLUSIONS

The discrete-time series modeling and identification of a lumped-mass rigid robotic joint with nonlinear dynamic friction have been proposed. The sliding dynamics, where the micro-displacement stiction force is already overcome, has been taken into consideration. The dynamic friction in sliding is approximated by a time lag transfer element in feedback, i.e. behind the static friction nonlinearity. The latter is described by means of a well-known Stribeck characteristic curve with partially linear parameters. The overall robot joint dynamics is transformed into the discrete-time representation, from which the corresponding regression model is derived. Both, the offline and online identification approaches have been formulated in the least-squares sense. Using the experimental setup of an industrial robotic manipulator the first vertical base-joint has been taken into consideration. Based on the collected high-noisy discrete-time data the identification has been accomplished in two stage. First, the Stribeck characteristic curve has been pre-estimated from the set of quasi-static drive experiments. This has been done in order to determine two exponential curvature parameters which are nonlinear and can not be included in the derived linear regression model. Afterwards, the sampled control and velocity signals from a multi-sinus reference trajectory have been used for the offline and online identification. The proposed modeling and identification method can be applied to a wide range of industrial and non-industrial robotic systems with nonlinear friction in the actuated joints. In the future works, the proposed modeling and identification approach will be extended to an adaptive, model-based control framework for compensating the dynamic friction.

ACKNOWLEDGMENT

The author acknowledges the laboratory support of Institute of Control Theory and System Engineering at TU-Dortmund by providing experiments with industrial robot.

REFERENCES

[1] C. Canudas De Wit, K. Astrom, and K. Braun, "Adaptive friction compensation in dc-motor drives," *IEEE Journal of Robotics and Automation*, vol. 3, no. 6, pp. 681–685, dec 1987.

[2] F. Altpeter, M. Grunenberg, P. Myszkorowski, and R. Longchamp, "Auto-tuning of feedforward friction compensation based on the gradient method," in *Proc. American Control Conference 2000*, vol. 4, 2000, pp. 2600–2604.

[3] H. S. Lee and M. Tomizuka, "Robust motion controller design for high-accuracy positioning systems," *IEEE Transactions on Industrial Electronics*, vol. 43, no. 1, pp. 48–55, feb 1996.

[4] M. Kermani, R. Patel, and M. Moallem, "Friction identification and compensation in robotic manipulators," *IEEE Transactions on Instrumentation and Measurement*, vol. 56, no. 6, pp. 2346–2353, dec. 2007.

[5] J. Swevers, C. Ganseman, D. Tukel, J. De Schutter, and H. Van Brussel, "Optimal robot excitation and identification," *IEEE Transactions on Robotics and Automation*, vol. 13, no. 5, pp. 730–740, oct 1997.

[6] A. Amthor, S. Zschaeck, and C. Ament, "High precision position control using an adaptive friction compensation approach," *IEEE Transactions on Automatic Control*, vol. 55, no. 1, pp. 274–278, 2010.

[7] D. Rizos and S. Fassois, "Friction identification based upon the LuGre and Maxwell Slip models," *IEEE Transactions on Control Systems Technology*, vol. 17, no. 1, pp. 153–160, jan 2009.

[8] E.-J. Kim, K. Seki, M. Iwasaki, and S.-H. Lee, "Modeling and identification of serial two-link manipulator considering joint nonlinearities for industrial robots control," in *Proc. IEEE/RSJ International Conference on Intelligent Robots and Systems (IROS2012)*, oct. 2012, pp. 2718–2723.

[9] M. Ruderman and T. Bertram, "FRF based identification of dynamic friction using two-state friction model with elasto-plasticity," in *Proc. IEEE International Conference on Mechatronics*, 2011, pp. 230–235.

[10] M. Ruderman, "Tracking control of motor drives using feed-forward friction observer (FFFO)," *IEEE Transactions on Industrial Electronics*, vol. PP, no. 99, pp. 1–1, 2013.

[11] T. Takemura and H. Fujimoto, "Simultaneous identification of linear parameters and nonlinear rolling friction for ball screw driven stage," in *Proc. 37th Annual Conference on IEEE Industrial Electronics Society (IECON 2011)*, nov. 2011, pp. 3424–3429.

[12] Y. Maeda and M. Iwasaki, "Rolling friction model-based analyses and compensation for slow settling response in precise positioning," *IEEE Transactions on Industrial Electronics*, vol. PP, no. 99, pp. 1–1, 2013.

[13] F. Al-Bender and J. Swevers, "Characterization of friction force dynamics," *IEEE Control Systems Magazine*, vol. 28, no. 6, pp. 64–81, 2008.

[14] L. Sciavicco and B. Siciliano, *Modelling and Control of Robot Manipulators*, 2nd ed. Berlin, Germany: Springer, 2000.

[15] M. Ruderman and T. Bertram, "Modeling and observation of hysteresis lost motion in elastic robot joints," in *Proc. 10th IFAC Symposium on Robot Control*, Sept. 2012, pp. 13–18.

[16] M. Ruderman and T. Bertram, "Two-state dynamic friction model with elasto-plasticity," *Mechanical Systems and Signal Processing*, vol. 39, no. 1–2, pp. 316–332, 2013.

[17] L. Ljung, "Recursive identification algorithms," *Circuits Systems Signal Processing*, vol. 21, no. 1, pp. 57–68, 2002.

[18] M. Morf, T. Kailath, and L. Ljung, "Fast algorithms for recursive identification," in *Proc. IEEE conference on Decision and Control including the 15th Symposium on Adaptive Processes*, vol. 15, Dec. 1976, pp. 916–921.

[19] M. Ruderman, F. Hoffmann, and T. Bertram, "Modeling and identification of elastic robot joints with hysteresis and backlash," *IEEE Transactions on Industrial Electronics*, vol. 56, no. 10, pp. 3840–3847, 2009.

[20] M. Ruderman, F. Hoffmann, and T. Bertram, "A Matlab-based framework for the remote control of a 6DOF robotic arm for education and research in control theory," in *Proc. IFAC 9th Symposium on Advances in Control Education (ACE2012)*, July 2012, pp. 366–371.

[21] M. Ruderman, F. Hoffmann, and T. Bertram, "Friction dynamic with elasto-plasticity in transient behavior," in *Proc. International Conference on Noise and Vibration Engineering (ISMA2010)*, Sept. 2010, pp. 1245–1258.